Distinguishing Highly Asymmetric Keratoconus Eyes Using Dual Scheimpflug/Placido Analysis

OREN GOLAN, ANDRE L. PICCININI, ERIC S. HWANG, ILDAMARIS MONTES DE OCA GONZALEZ, MARK KRAUTHAMMER, SUMITRA S. KHANDELWAL, DAVID SMADJA, AND J. BRADLEY RANDLEMAN

• PURPOSE: To identify the best metrics or combination of metrics that provide the highest predictive power between normal eyes and the clinically unaffected eye of patients with highly asymmetric keratoconus using data from a Dual Scheimpflug/Placido device.

• DESIGN: Retrospective case-control study.

• METHODS: Combined Dual Scheimpflug/Placido imaging was obtained from the Galilei G4 device (Ziemer Ophthalmic Systems AG, Port, Switzerland) in 31 clinically unaffected eyes with highly asymmetric keratoconus and 178 eyes from 178 patients with bilaterally normal corneal examinations that underwent uneventful LASIK with at least 1 year follow-up. Receiver operating characteristic (ROC) curves were generated to determine area under the curve (AUC), sensitivity, and specificity for 87 metrics, and logistic regression modeling was used to determine optimal variable combinations.

• RESULTS: No individual metric achieved an AUC greater than 0.79. A combined model consisting of 9 metrics yielded an AUC of 0.96, with 90.3% sensitivity and 92.6% specificity. Among those 9 metrics included, 5 related to corneal pachymetry: Opposite Sector Index and Anterior Height BFS Z from the anterior surface, Asphericity and Asymmetry Index, Posterior Height BFS Z, and Posterior Height BFS X from the posterior surface. The strongest variable in the model was the thinnest point location on the horizontal (x) axis.

• CONCLUSION: While individual metrics performed poorly, using a combination of metrics from the combined Dual Scheimpflug/Placido device provided a useful model for differentiating normal corneas from the clinically normal eyes of patients with highly asymmetric keratoconus. Pachymetry values were the most impactful metrics. (Am J Ophthalmol 2019;201:46–53. © 2019 Elsevier Inc. All rights reserved.)

AJO.com Supplemental Material available at AJO.com.
Accepted for publication Jan 22, 2019.

From the Keck School of Medicine of the University of Southern California, Los Angeles, California, USA (O.G., A.L.P., E.S.H., J.B.R.); Tel Aviv Souraski Medical Center, Tel Aviv University, Tel Aviv, Israel (O.G., M.K.); Sadalla Amin Ghanem Eye Hospital, Joinville, Santa Catarina, Brazil (A.L.P.); Cullen Eye Institute, Baylor College of Medicine, Houston, Texas, USA (I.M.G., S.S.K.); Department of Ophthalmology, Shaare Zedek Medical Center, Jerusalem, Israel (D.S.); and USC Roski Eye Institute, Los Angeles, California, USA (J.B.R.).

Inquiries to J. Bradley Randleman, Keck School of Medicine, 1450 San Pablo St, Los Angeles, CA 90033, USA; e-mail: randlema@usc.edu

SCREENING FOR SIGNS OF KERATOCONUS (KC) AND related corneal ectatic disorders in the earliest stages remains challenging, and identification using a single device[1–8] or a combination of different technologies[9,10] still remains suboptimal. Corneal ectasia after excimer laser refractive surgery is a rare but still serious complication that can arise, with a higher probability in eyes with undiagnosed early signs of keratoconus.[11–13]

Initially, most screening for KC detection was performed using Placido reflection-based technology to evaluate anterior surface curvature.[13–19] With the evolution of corneal tomography, multiple devices have the ability to measure additional variables such as regional corneal thickness and anterior and posterior surface elevation. Varying technologies use scanning-slit beam imaging, Scheimpflug technology, combined Scheimpflug and Placido imaging, and combined Dual Scheimpflug imaging and Placido imaging.

The optimal metric or group of metrics to use for KC detection is still greatly debated in the literature, as some authors suggest that earliest signs of keratoconus can be identified using corneal thickness variables[20–22] while other suggest that changes first manifest in posterior corneal surface maps.[3,23,24] Various studies have combined multiple variables from the anterior and posterior surfaces to achieve better predicative models, while other groups have used wavefront aberration metrics[1,25–29] or optical coherence tomography (OCT)-derived corneal thickness changes and epithelial thickness distribution maps.[30] There are also devices that aim to measure the corneal biomechanical strength directly.[31–34] To date, none of these individual technologies has been established as optimal or superior to other technologies in identifying keratoconus in its earliest stages.

The purpose of this study was to identify the variables and variable combinations most impactful in differentiating normal control eyes from the minimally affected eye of patients with highly asymmetric keratoconus using a Dual Scheimpflug/Placido-based imaging device.

METHODS

THIS RETROSPECTIVE, CASE-CONTROLLED STUDY WAS CONducted at the Department of Ophthalmology, Keck School of Medicine, University of South California, Los Angeles, California, USA, and approved separately by the

0002-9394/$36.00
https://doi.org/10.1016/j.ajo.2019.01.023

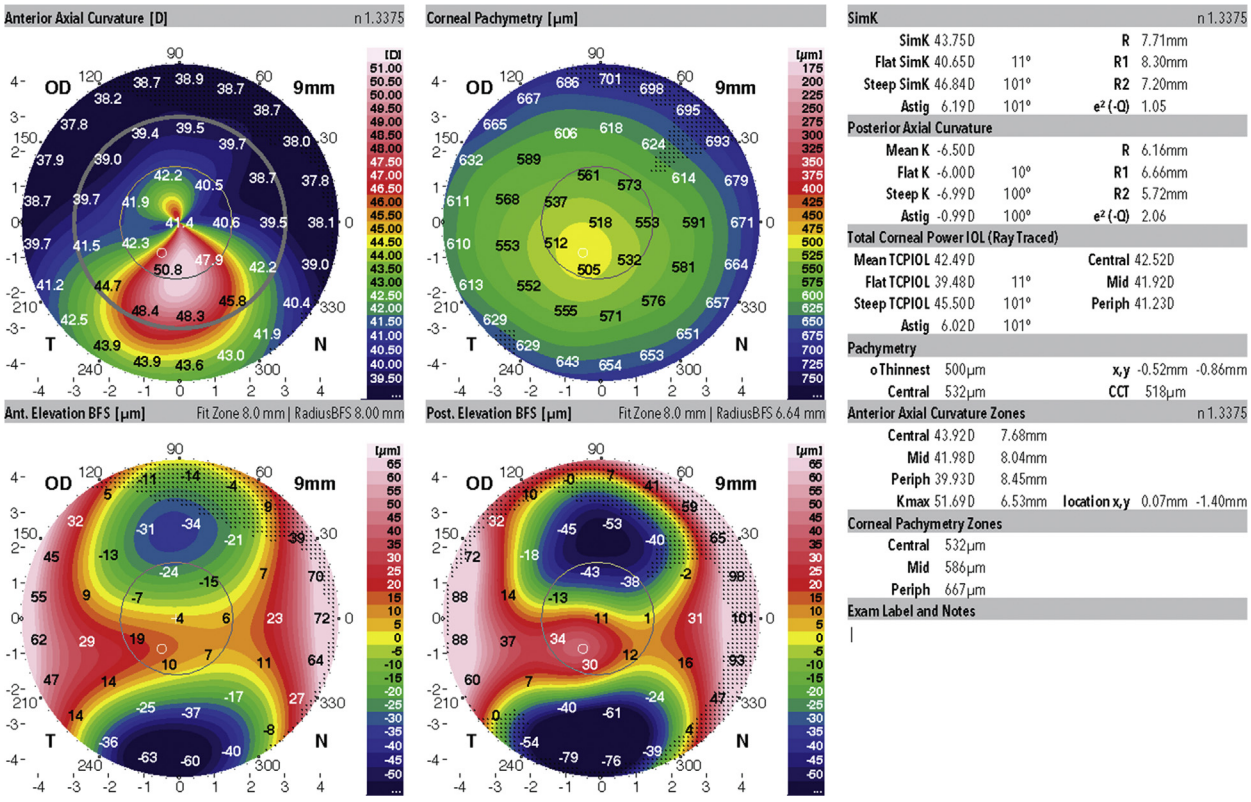

FIGURE 1. Representative Dual Scheimpflug/Placido image from the clinically affected keratoconus eye of a patient from this study.

Institutional Review Boards of Emory University (Atlanta, Georgia, USA), Baylor College of Medicine (Houston, Texas, USA), and the University of Southern California (Los Angeles, California, USA). The study was conducted in accordance with the tenets of the Declaration of Helsinki.

The study and population presented to Emory University, Baylor College of Medicine, and the Tel Aviv Sourasky Medical Center (Tel Aviv, Israel) from 2014 to 2017. Patients were included in the study group if they had highly asymmetric keratoconus disease presentation. Specifically, all study patients had clear evidence of keratoconus in 1 eye and no clear evidence of disease in the clinically unaffected eye. For the clinically involved eye, all 31 affected fellow eyes were identified using this screening methodology; patients had abnormal focal anterior corneal steepening, focal corneal thinning, clinical evidence of disease at the slit lamp, scissoring on retinoscopy, subjectively impaired visual acuity, and best corrected distance visual acuity (CDVA) worse than 20/20. For the unaffected asymmetric keratoconus eye (AKC), there were the following features: no clinical evidence of disease, no physical findings on slit-lamp examination, no definitive abnormalities on corneal imaging, and CDVA of 20/20 or better. All image screening was performed directly on the computer using a variety of settings and review of different maps; thus no one single output style was relied upon for image screening. Representative study population images are shown for the AKC group in Figures 1 and 2. The complete set of Dual Scheimpflug/Placido imaging is available as supplemental images (Supplemental Material available at AJO.com).

The control group comprised patients with preoperative bilateral normal topography and tomography maps who all underwent LASIK at Emory with at least 1 year uneventful follow-up (Figure 3). Eyes with ocular pathology, previous ocular surgery, soft contact lenses worn 1 week before or rigid contact lens 2 weeks before, and low-quality topography maps that did not fulfill the minimal quality required by the system were excluded from analysis.

• **DUAL SCHEIMPFLUG/PLACIDO DEVICE PARAMETERS:** All measurements were performed with the Galilei Dual Scheimpflug Analyzer (G2 and G4; Ziemer Ophthalmic Systems AG, Port, Switzerland) according to the manufacturer's instructions. The Galilei device is a combined Placido topography and Scheimpflug tomography device with a Dual Scheimpflug camera. The system obtains between 15 and 60 Scheimpflug images each scan and 2 Placido top view images at 90 degrees apart, while the cameras rotate over a central axis. Scheimpflug and Placido data are obtained concurrently. Data extrapolated from the Scheimpflug and Placido images are merged to deliver a

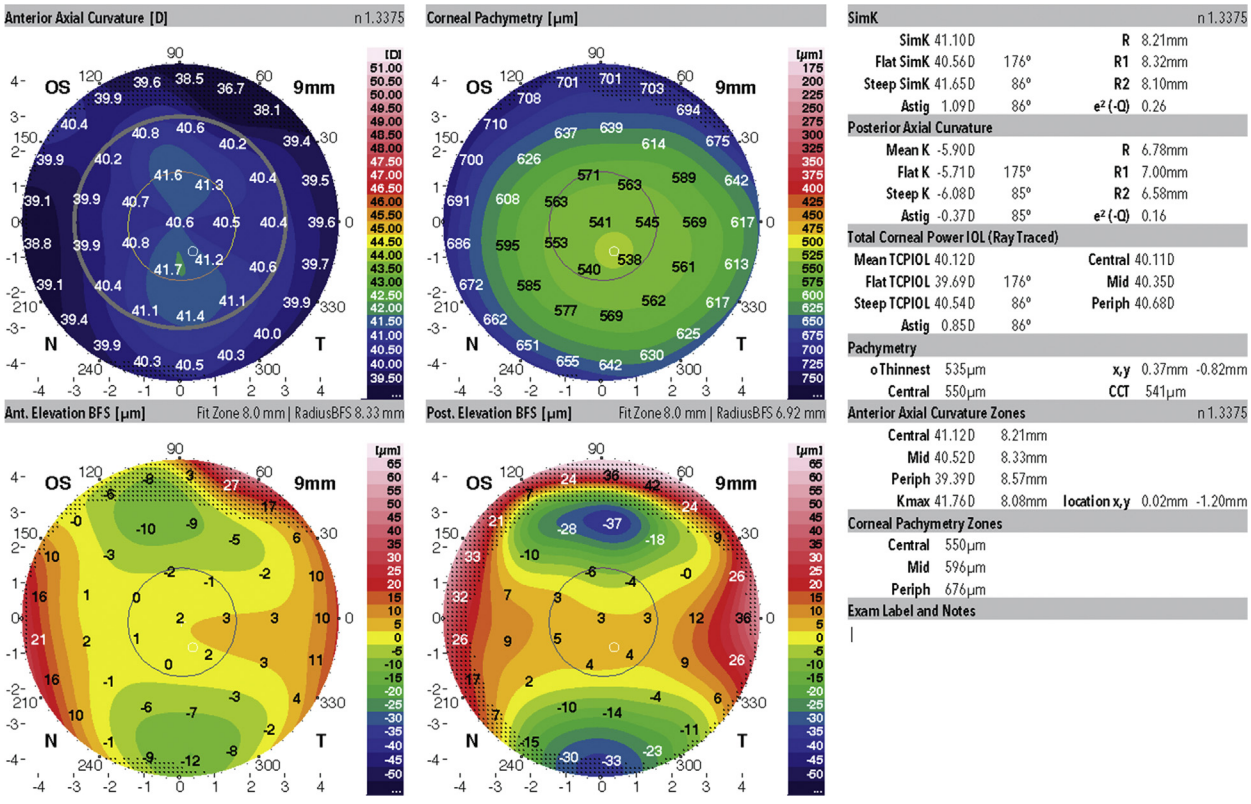

FIGURE 2. Representative Dual Scheimpflug/Placido image from the clinically unaffected eye (subclinical asymmetric keratoconus); fellow eye from the same patient shown in Figure 1.

surface tailored to the anterior cornea. Data from the posterior corneal surface is measured using the edge detection in images provided by the Dual Scheimpflug system. The devices used in this study were set up using the standard settings to acquire 15 images.

The analysis was performed with the Galilei device's software version 6.3.1b3 (Ziemer Ophthalmic Systems AG, Port, Switzerland). A total of 87 corneal metrics was collected for the analysis. The majority of the metrics were exported automatically by the Galilei software to csv files except for the high-order aberrations, the elevation data from the best fit sphere (BFS) maps, best fit toric and aspheric (BFTA) maps, and the Posterior Asymmetry and Asphericity index (AAI) that were collected automatically but exported manually. The Posterior AAI was obtained through manual calculations as previously described.[35,36] The Posterior AAI is calculated using the BFTA map as the absolute value of the highest negative elevation and highest positive elevation value within the posterior central 6-mm-diameter data zone, 180 degrees opposite 45-degree zones (Figure 4).

• **STATISTICAL ANALYSIS:** Differences between the data were evaluated using the Levene test for equality of variance and the Student 2-sample *t* test. Owing to the high number of corneal metrics analyzed, the level of significance was adjusted with Bonferroni correction and set to $P < .0005$ for individual variables. Data were expressed as mean and standard deviation (SD). Receiver operating characteristics (ROC) curves were used to assess the discriminating ability and to determine the optimal cutoff values for each significant metric and multivariable combination. Cutoff points were calculated using the Youden index. After collection of all significant metrics, for the logistic regression, Wald's χ^2 test was used to reach the strongest influential combination of variables in a stepwise manner to produce maximal area under ROC curve (AUROC) values using least number of variables. The statistical analysis was performed using the SPSS software, version 24 (IBM Corp, Armonk, New York, USA).

RESULTS

THIS STUDY INCLUDED 31 HIGHLY ASYMMETRIC, CLINIcally normal fellow eyes from 31 patients with definitive keratoconus in the contralateral eye (AKC group) and 178 eyes from 178 bilaterally normal control patients (Control group). There were no significant differences

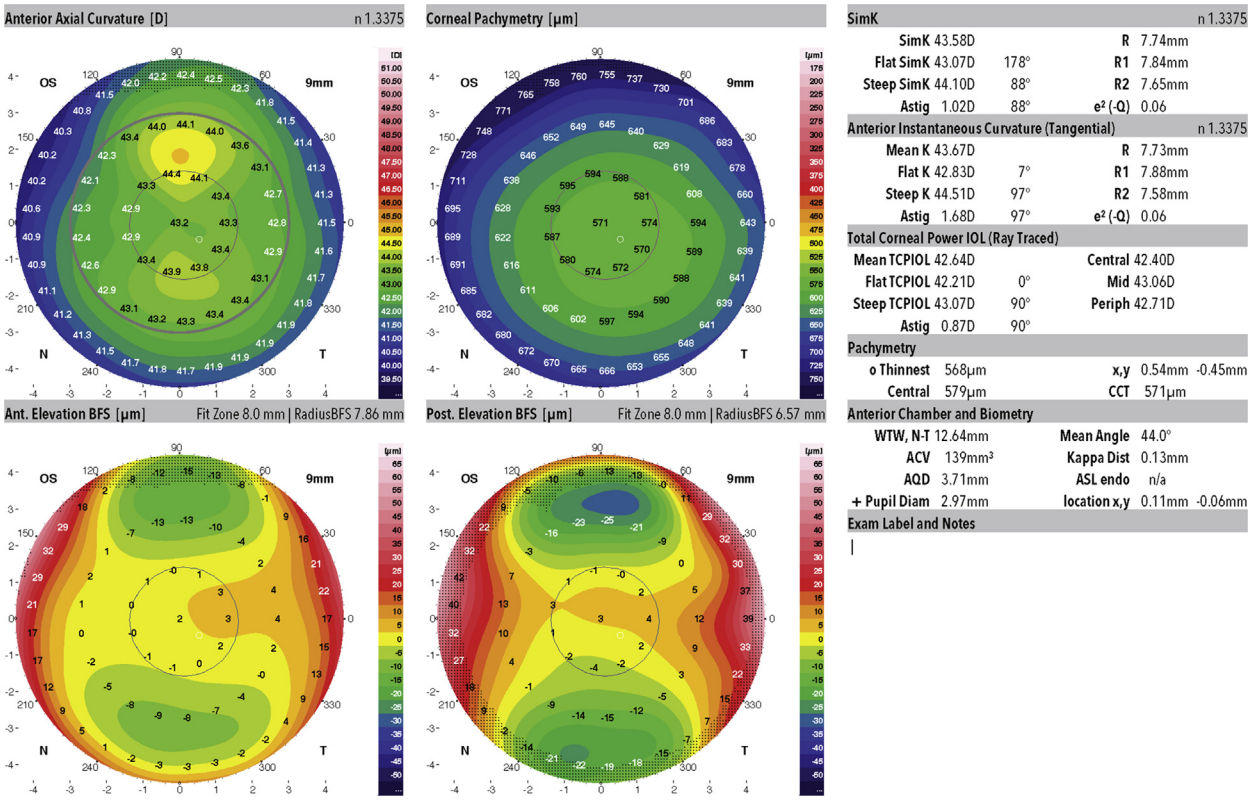

FIGURE 3. Representative Dual Scheimpflug/Placido image from a bilaterally normal topography and tomography eye of a patient from this study.

between groups for age 31.87 ± 8.57 years (range 17-71 years) AKC vs. 28.74 ± 16.55 years (range 20-71 years) Control ($P > .05$). The percentage of male subjects was significantly higher in the AKC group than the Control group (71% male in AKC vs 48.3% male in Controls group; $P = .02$). Mean anterior surface astigmatism value was 0.95 ± 0.41 diopter (D) in the AKC group compared to 0.85 ± 0.61 D in the Control group ($P > .05$) and mean anterior surface inferior-superior ratio was 0.65 ± 0.42 D in the AKC group and 0.65 ± 0.42 D in the Control group ($P > .05$).

Out of 87 corneal metrics analyzed, 10 were found to be highly significantly different between groups, with the Student *t* test value after Bonferroni correction of $P < .000574$. None of the keratoconus probability metrics (KPI, KPROB, CLMIaa, PPK) were significant ($P > .05$). Out of the 10 significant metrics, none had an independent strong predictive value; the strongest independent value was the corneal location of the thinnest point on the x-axis (AUC = 0.794) (Table 1). Five of the 10 highly significant metrics were related to pachymetry. Significant anterior surface metrics included the Opposite Sector Index (OSI) and Anterior Height BFS Z, while significant posterior surface metrics included the AAI, Posterior Height BFS Z, and Posterior Height BFS X. The BFS Z anterior and posterior height metrics represent the exact machine coordinate of the distance of the center of the BFS from the Placido disc in the Z direction, while the Posterior Height X describes how far the center of the BFS is away from the measurement Scheimpflug camera head's rotation axis.

The best combination in logistic regression modeling was achieved with a combination of 9 metrics (Table 2). The model predictive power had a 0.961 AUROC, sensitivity of 90.3%, and specificity of 92.6%. The most significant variables in modeling were pachymetry metrics, while the least impactful, though still relevant, were the anterior and posterior BFS Z variables.

DISCUSSION

IN THIS STUDY WE FOUND THAT ALTHOUGH NO INDIVIDUAL metric performed well in discriminating between clinically unaffected eyes from patients with highly asymmetric keratoconus and normal corneas, a combination of anterior surface, posterior surface, and corneal thickness metrics yielded a good predictive model.

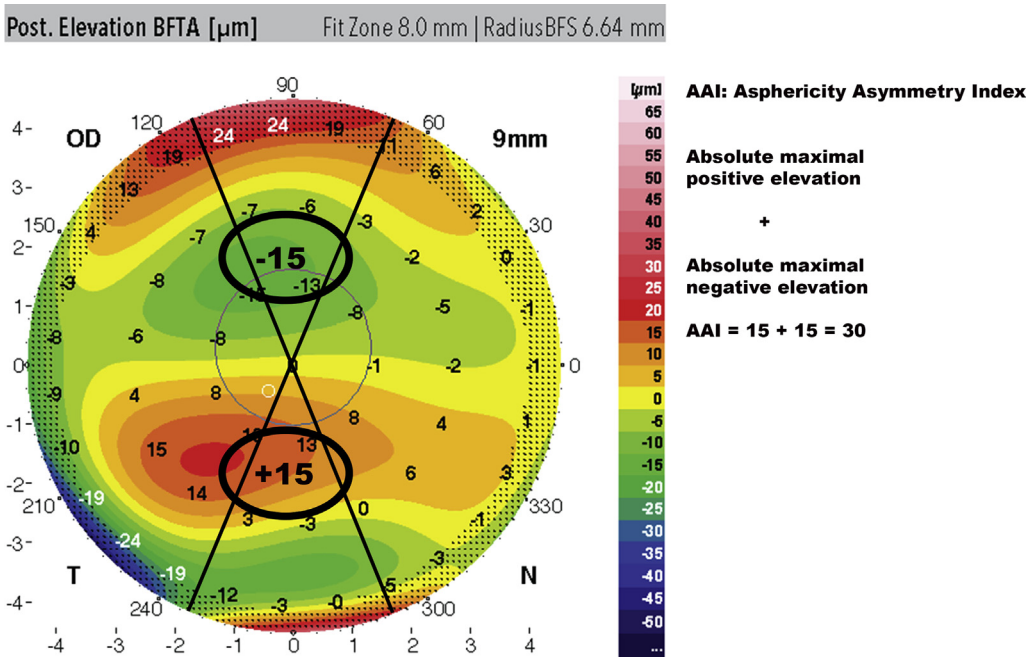

FIGURE 4. Asphericity Asymmetry Index (AAI) calculation. Adding the absolute value of the maximum positive elevation and the maximum negative depression values within the 6 mm zone of the best fit toric aspheric (BFTA) posterior elevation map in 180 degrees opposite 45-degree zones yields the AAI. In this example, AAI = +15 + (15) = 30.

The majority and most significant metrics of this model were related to corneal pachymetry. In this study 5 out of 9 metrics in the model were related to corneal pachymetry and volume. The significance of corneal thickness and corneal volume in the detection of subclinical keratoconus has been reported before, both in subclinical keratoconus and in keratoconic eyes, demonstrating a relative thinner cornea with a reduced corneal volume.[5,20–22,24,37] Metrics used from the posterior surface were the AAI along with the machine coordinate of the distance between the center of the BFS from the Placido disc in the Z direction (Posterior Height BFS Z). Metrics from the anterior surface were the Irregular Astigmatism Index, which is an objective, machine-derived variable calculated as the difference between average dioptric values in the inferior and superior areas within the 3 mm corneal vertex, and the machine coordinate of the distance of the central BFS from the Placido disc in the Z axis (Anterior Height BFS Z). The most significant metric in the logistic regression model was the location of the thinnest point temporally on the horizontal (x) axis. The thinnest point on the y-axis was also highly significant; however, its contribution to the logistic regression model was negligible. The OSI was highly significant but did not contribute to the final model.

The posterior AAI is a relatively new, manually derived metric used as a quantitative indicator of the asymmetry and asphericity of the posterior corneal surface. A similar type of index was identified by Nilforoushan and associates in studies using Scheimpflug imaging and was found to be predictive for subclinical keratoconus when combined with other variables.[38] The variable, "high minus low," was created from the difference between the highest and lowest points on the posterior elevation within the central posterior 7 mm zone.[38] Bae and associates similarly calculated posterior elevation difference (max-min) for Scheimpflug imaging and found a calculated AUROC of 0.735, although in that study anterior surface curvature variables were best at distinguishing populations.[18] In a recent study by Smadja and associates, the posterior AAI was selected by an automated decision tree classifier to be the most discriminative variable to differentiate between normal and subclinical keratoconus eyes out of 55 evaluated metrics.[35] In that study the cutoff point between subclinical KC and normal eyes was estimated as 21.5, while in this study the optimal value was 13.5, which yielded an AUC of 0.750, with 77% sensitivity and 67% specificity. This discrepancy between studies could be owing to the fact that the AAI is still not incorporated into the device's analyzer and had to be calculated manually and thereby is prone to subjective evaluation differences. Ambrosio and associates reported a sensitivity of 80% and specificity of 70% for the Belin/Ambrosio Deviation score (BAD-D) index for distinguishing normal eyes from the uninvolved fellow eye of highly asymmetric keratoconus.[34] The sensitivity and specificity improved to 90% and 96%, respectively, using a novel Tomographic and Biomechanical Index, which combines BAD-D with

TABLE 1. Dual Scheimpflug/Placido Variables That Were Significantly Different Between Asymmetric Keratoconus and Control Study Populations

Variable	Control	AKC	*P* Value	AUC	95% CI	Cutoff	Sensitivity	Specificity
Anterior Height BFS Z (mm)	34.36 ± 0.39 (33.32-35.2)	34.02 ± 0.42 (33.03-34.88)	.000006	0.723	0.625-0.821	33.96	51.6%	84.8%
OSI [D]	0.76 ± 0.33 (0.12-1.6)	1.02 ± 0.55 (0.22-3.07)	.00777	0.658	0.203-0.405	0.671	83.9%	45%
Posterior Height BFS X (mm)	-0.03 ± 0.02 (-0.11 to 0.04)	0.0025 ± 0.04 (-0.07 to 0.07)	.000008	0.764	0.658-0.879	-0.01	61.3%	87%
Posterior Height BFS Z (mm)	35.05 ± 0.36 (33.9-35.9)	34.78 ± 0.39 (33.86-35.58)	.000008	0.696	0.595-0.797	34.97	71%	61.2%
Central corneal pachymetry 0-4 mm (μm)	563 ± 26 (505-621)	542 ± 27 (490-611)	.00382	0.701	0.603-0.800	543	58%	75.8%
Central corneal pachymetry 2 mm (μm)	555 ± 26 (500-613)	533 ± 27 (482-598)	.000038	0.716	0.619-0.813	534	58%	77.5%
Thinnest corneal value (μm)	553 ± 26 (498-612)	529 ± 27 (470-595)	.000001	0.733	0.640-0.827	553	87%	48.8%
Thinnest pachymetry location x-axis	-0.50 ± 0.24 (-1.49 to 0.44)	0.04 ± 0.55 (-1.04 to 1.1)	.000002	0.794	0.682-0.906	-0.15	64.5%	94.3%
Thinnest pachymetry location y-axis	-0.26 ± 0.23 (-0.98 to 0.28)	-0.52 ± 0.24 (-1.2 to -0.13)	.0000000036	0.784	0.703-0.865	-0.41	71%	75%
AAI	12.46 ± 5.73 (4-38)	18.54 ± 7.8 (6-38)	.00011	0.750	0.658-0.841	13.50	77.4%	67%
IAI	0.42 ± 0.03 (0.35-0.54)	0.411 ± 0.038 (0.32-0.50)	.01	0.625	0.519-0.730	0.4	51.6%	73.6%
Corneal volume (mm^3)	31.61 ± 1.58 (27-35)	30.81 ± 1.57 (27.5-34.6)	.0047	0.640	0.549-0.740	30	42%	82%

AAI = Posterior Surface Asphericity Asymmetry Index; AKC = highly asymmetric keratoconus group; AUC = area under the curve; IAI = Anterior Surface Irregular Astigmatism Index; OSI = Anterior Surface Opposite Sector Index.

metrics from a biomechanical evaluation from the Corvis-ST device.

In our study the IAI had an AUROC of 0.625 with a 51.6% sensitivity and 73.6% specificity and an optimal cutoff value of 0.4. This result approximately agrees with Feizi and associates, who found AUROC of 0.664 for a cutoff point of 0.445.[39] Shetty and associates found better predictive ability with a similar cutoff value of 0.45 (AUROC 0.858, 54% sensitivity, 81.4% specificity).[40] The differences in predictive power between studies may be owing in part to differing classifications of description asymmetric (subclinical) disease, as the eyes in the study by Shetty included eyes with asymmetric bowtie and skewed radial axis patterns.

In this study none of the higher-order aberrations (HOA) were significantly different between groups. Saad and Gatinel used a combined Placido disk and wavefront aberrometry device based on dynamic skiascopy (OPD-Scan; Nidek Co Ltd, Gamagori, Japan) to create a model that combined 4 HOA metrics along with 4 Placido disc metrics to identify subclinical keratoconus. A sensitivity and specificity pair of 89% and 92% were calculated, though a sensitivity of 63% was recalculated in their validation study.[25] Bühren used a scanning slit system (Orbscan IIz; Bausch & Lomb, Rochester, New York, USA) to combine HOA metrics from both anterior and posterior corneal surfaces in addition to thickness data to achieve an AUROC of 0.857 and sensitivity/specificity pair of 68.8% and 95.1%, respectively, in the validation group.[1,41] Reddy and associates evaluated HOA extrapolated by the Dual Scheimpflug analyzer (Galilei) and found that third-order HOA and Total RMS were the most significant (AUROC of 0.83 and 0.82, respectively); however, eyes in the subclinical KC group included ones with maps containing skewed anterior radial axes, which have the potential to induce HOA.[19] A study using a combination of corneal and total ocular HOA reached a sensitivity and specificity of 91% and 94%, respectively.[26] Taken together, these results support our findings that corneal HOA are not particularly predictive in early stages of keratoconus.

While the multivariable model in our study achieved a predictive value of 90% sensitivity and 92% specificity, recent work from our group achieved 100% sensitivity and 100% specificity in a similar study population using a combination of metrics from spectral-domain OCT (SDOCT) and Scheimpflug imaging.[42] That study used 2 separate technologies and incorporated epithelial thickness parameters. Metrics reporting epithelial thickness variability were found to be highly significant and important for optimal modeling to distinguish the study populations. Those epithelial metrics were not available in this cohort and may have further delineated the groups. While the studies were performed in unique cohorts and were therefore not directly comparable, the optimal model achieved using combined Dual

TABLE 2. Variable Rank by Impact on Combined Variable Model to Distinguish Between Asymmetric Keratoconus and Control Study Populations

	Wald Value	9-Variable Model
Variable rank		
1	15.285	Thinnest pachymetry location on the x-axis
2	9.778	Thinnest pachymetry value
3	5.629	Average central 2 mm pachymetry
4	5.314	IAI
5	2.927	AAI
6	1.860	Corneal volume (mm^3)
7	1.352	Average middle 4-7 mm pachymetry
8	1.215	Posterior Height BFS Z
9	0.948	Anterior Height BFS Z
AUC		0.961
Sensitivity		90.3%
Specificity		92.6%

AAI = posterior surface Asphericity Asymmetry Index; AUC = area under the curve; BFS Z = best fit sphere in the z direction; IAI = anterior surface Irregular Astigmatism Index.

Scheimpflug/Placido imaging in this study performed slightly better than optimal models from either SD-OCT imaging only (89% specificity, 89% sensitivity) or Scheimpflug imaging only (83% specificity, 83% sensitivity) models from the previous work. We looked at all false-positive and false-negative cases in detail after analysis but could not discern any specific pattern or deviation that specifically contributed to their misclassification.

Limitations in this study include small sample size and lack of long-term follow-up. Lack of follow-up or intervention in these eyes limits our ability to identify parameters that best indicate a higher risk of keratoconus progression. The cases were obtained from multiple locations and as such do not represent a specific geographic cohort. As patients with highly asymmetric keratoconus represent a heterogenous cohort, we anticipate that a similar analysis performed in a different group may find a slightly different combination of optimal variables; however, we predict that future optimal models using Dual Scheimpflug/Placido technology will include pachymetry measures as well as anterior and posterior surface asymmetry metrics. Finally, none of the metrics identified directly measure corneal biomechanics; rather, they all describe corneal morphology.

In conclusion, our findings demonstrate that the clinically unaffected fellow eye in patients with highly asymmetric keratoconus remains challenging to identify using any individual metric from Dual Scheimpflug/Placido imaging; however, a combination of metrics, weighted heavily toward pachymetric variables, yielded good discriminative power.

FUNDING/SUPPORT: SUPPORTED BY NIH GRANT R01 EY028666 (J.B.R.) AND SEPARATE UNRESTRICTED DEPARTMENTAL GRANTS to the USC Roski Eye Institute, and Baylor College of Medicine/Cullen Eye Institute from Research to Prevent Blindness (New York, New York, USA). Financial Disclosures: David Smadja is a paid consultant for Ziemer Ophthalmic System AG. The following authors have no financial disclosures: Oren Golan, Andre L. Piccinini, Eric S. Hwang, Ildamaris Montes De Oca Gonzalez, Mark Krauthammer, Sumitra S. Khandelwal, and J. Bradley Randleman. All authors attest that they meet the current ICMJE criteria for authorship.

REFERENCES

1. Buhren J, Kook D, Yoon G, Kohnen T. Detection of subclinical keratoconus by using corneal anterior and posterior surface aberrations and thickness spatial profiles. *Invest Ophthalmol Vis Sci* 2010;51(7):3424–3432.
2. Cui J, Zhang X, Hu Q, Zhou WY, Yang F. Evaluation of corneal thickness and volume parameters of subclinical keratoconus using a Pentacam Scheimpflug system. *Curr Eye Res* 2016;41(7):923–926.
3. de Sanctis U, Loiacono C, Richiardi L, Turco D, Mutani B, Grignolo FM. Sensitivity and specificity of posterior corneal elevation measured by Pentacam in discriminating keratoconus/subclinical keratoconus. *Ophthalmology* 2008;115(9):1534–1539.
4. Jia Y, Zhu H, Zhou J. Pentacam scheimpflug tomography findings in topographically normal patients and subclinical keratoconus cases. *Am J Ophthalmol* 2015;159(1):209.
5. Ruisenor Vazquez PR, Galletti JD, Minguez N, et al. Pentacam Scheimpflug tomography findings in topographically normal patients and subclinical keratoconus cases. *Am J Ophthalmol* 2014;158(1):32–40.e32.
6. Smadja D, Santhiago MR, Mello GR, Krueger RR, Colin J, Touboul D. Influence of the reference surface shape for discriminating between normal corneas, subclinical keratoconus, and keratoconus. *J Refract Surg* 2013;29(4):274–281.
7. Steinberg J, Aubke-Schultz S, Frings A, et al. Correlation of the KISA% index and Scheimpflug tomography in 'normal', 'subclinical', 'keratoconus-suspect' and 'clinically manifest' keratoconus eyes. *Acta Ophthalmol* 2015;93(3):e199–e207.
8. Ucakhan OO, Cetinkor V, Ozkan M, Kanpolat A. Evaluation of Scheimpflug imaging parameters in subclinical keratoconus, keratoconus, and normal eyes. *J Cataract Refract Surg* 2011;37(6):1116–1124.
9. Luz A, Lopes B, Hallahan KM, et al. Enhanced combined tomography and biomechanics data for distinguishing forme fruste keratoconus. *J Refract Surg* 2016;32(7):479–494.
10. Rabinowitz YS, Li X, Canedo AL, Ambrosio R Jr, Bykhovskaya Y. Optical coherence tomography combined with videokeratography to differentiate mild keratoconus subtypes. *J Refract Surg* 2014;30(2):80–87.

11. Randleman JB, Russell B, Ward MA, Thompson KP, Stulting RD. Risk factors and prognosis for corneal ectasia after LASIK. *Ophthalmology* 2003;110(2):267–275.
12. Randleman JB, Trattler WB, Stulting RD. Validation of the Ectasia Risk Score System for preoperative laser in situ keratomileusis screening. *Am J Ophthalmol* 2008;145(5):813–818.
13. Randleman JB, Woodward M, Lynn MJ, Stulting RD. Risk assessment for ectasia after corneal refractive surgery. *Ophthalmology* 2008;115(1):37–50.
14. Rabinowitz YS, Rasheed K. KISA% index: a quantitative videokeratography algorithm embodying minimal topographic criteria for diagnosing keratoconus. *J Cataract Refract Surg* 1999;25(10):1327–1335.
15. Li X, Yang H, Rabinowitz YS. Longitudinal study of keratoconus progression. *Exp Eye Res* 2007;85(4):502–507.
16. Li X, Rabinowitz YS, Rasheed K, Yang H. Longitudinal study of the normal eyes in unilateral keratoconus patients. *Ophthalmology* 2004;111(3):440–446.
17. Klyce SD, Karon MD, Smolek MK. Screening patients with the corneal navigator. *J Refract Surg* 2005;21(5 Suppl): S617–S622.
18. Bae GH, Kim JR, Kim CH, Lim DH, Chung ES, Chung TY. Corneal topographic and tomographic analysis of fellow eyes in unilateral keratoconus patients using Pentacam. *Am J Ophthalmol* 2014;157(1):103–109.e101.
19. Reddy JC, Rapuano CJ, Cater JR, Suri K, Nagra PK, Hammersmith KM. Comparative evaluation of dual Scheimpflug imaging parameters in keratoconus, early keratoconus, and normal eyes. *J Cataract Refract Surg* 2014;40(4):582–592.
20. Ambrosio R Jr, Caiado AL, Guerra FP, et al. Novel pachymetric parameters based on corneal tomography for diagnosing keratoconus. *J Refract Surg* 2011;27(10):753–758.
21. Ambrosio R Jr, Alonso RS, Luz A, Coca Velarde LG. Corneal-thickness spatial profile and corneal-volume distribution: tomographic indices to detect keratoconus. *J Cataract Refract Surg* 2006;32(11):1851–1859.
22. Saad A, Gatinel D. Topographic and tomographic properties of forme fruste keratoconus corneas. *Invest Ophthalmol Vis Sci* 2010;51(11):5546–5555.
23. Schlegel Z, Hoang-Xuan T, Gatinel D. Comparison of and correlation between anterior and posterior corneal elevation maps in normal eyes and keratoconus-suspect eyes. *J Cataract Refract Surg* 2008;34(5):789–795.
24. Pinero DP, Alio JL, Aleson A, Escaf Vergara M, Miranda M. Corneal volume, pachymetry, and correlation of anterior and posterior corneal shape in subclinical and different stages of clinical keratoconus. *J Cataract Refract Surg* 2010;36(5): 814–825.
25. Saad A, Gatinel D. Combining placido and corneal wavefront data for the detection of forme fruste keratoconus. *J Refract Surg* 2016;32(8):510–516.
26. Saad A, Gatinel D. Evaluation of total and corneal wavefront high order aberrations for the detection of forme fruste keratoconus. *Invest Ophthalmol Vis Sci* 2012;53(6):2978–2992.
27. Jafri B, Li X, Yang H, Rabinowitz YS. Higher order wavefront aberrations and topography in early and suspected keratoconus. *J Refract Surg* 2007;23(8):774–781.
28. Colak HN, Kantarci FA, Yildirim A, et al. Comparison of corneal topographic measurements and high order aberrations in keratoconus and normal eyes. *Cont Lens Anterior Eye* 2016;39(5):380–384.
29. Buhren J, Kuhne C, Kohnen T. Defining subclinical keratoconus using corneal first-surface higher-order aberrations. *Am J Ophthalmol* 2007;143(3):381–389.
30. Temstet C, Sandali O, Bouheraoua N, et al. Corneal epithelial thickness mapping using Fourier-domain optical coherence tomography for detection of form fruste keratoconus. *J Cataract Refract Surg* 2015;41(4):812–820.
31. Vinciguerra R, Ambrosio R Jr, Roberts CJ, Azzolini C, Vinciguerra P. Biomechanical characterization of subclinical keratoconus without topographic or tomographic abnormalities. *J Refract Surg* 2017;33(6):399–407.
32. Scarcelli G, Besner S, Pineda R, Yun SH. Biomechanical characterization of keratoconus corneas ex vivo with Brillouin microscopy. *Invest Ophthalmol Vis Sci* 2014;55(7): 4490–4495.
33. Scarcelli G, Besner S, Pineda R, Kalout P, Yun SH. In vivo biomechanical mapping of normal and keratoconus corneas. *JAMA Ophthalmol* 2015;133(4):480–482.
34. Ambrosio R Jr, Lopes BT, Faria-Correia F, et al. Integration of Scheimpflug-based corneal tomography and biomechanical assessments for enhancing ectasia detection. *J Refract Surg* 2017;33(7):434–443.
35. Smadja D, Touboul D, Cohen A, et al. Detection of subclinical keratoconus using an automated decision tree classification. *Am J Ophthalmol* 2013;156(2): 237–246.e231.
36. Golan O, Hwang ES, Lang P, et al. Differences in posterior corneal features between normal corneas and subclinical keratoconus. *J Refract Surg* 2018;34(10):664–670.
37. Tellouck J, Touboul D, Santhiago MR, Tellouck L, Paya C, Smadja D. Evolution profiles of different corneal parameters in progressive keratoconus. *Cornea* 2016;35(6): 807–813.
38. Nilforoushan MR, Speaker M, Marmor M, et al. Comparative evaluation of refractive surgery candidates with Placido topography, Orbscan II, Pentacam, and wavefront analysis. *J Cataract Refract Surg* 2008;34(4):623–631.
39. Feizi S, Yaseri M, Kheiri B. Predictive ability of Galilei to Distinguish subclinical keratoconus and keratoconus from normal corneas. *J Ophthalmic Vis Res* 2016;11(1):8–16.
40. Shetty R, Rao H, Khamar P, et al. Keratoconus screening indices and their diagnostic ability to distinguish normal from ectatic corneas. *Am J Ophthalmol* 2017;181:140–148.
41. Buhren J, Schaffeler T, Kohnen T. Validation of metrics for the detection of subclinical keratoconus in a new patient collective. *J Cataract Refract Surg* 2014;40(2): 259–268.
42. Hwang E, Perez-Straziota C, Kim S, Santhiago M, Randleman J. Distinguishing highly asymmetric keratoconus eyes using combined Scheimpflug and spectral domain OCT analysis. *Ophthalmology* 2018;125(12): 1862–1871.